

# Segment Anything Model for Medical Image Analysis: an Experimental Study

Maciej A. Mazurowski<sup>1,2,3,4</sup> Haoyu Dong<sup>2</sup> Hanxue Gu<sup>2</sup>

Jichen Yang<sup>2</sup> Nicholas Konz<sup>2</sup> Yixin Zhang<sup>2</sup>

<sup>1</sup> Department of Radiology <sup>2</sup> Department of Electrical and Computer Engineering

<sup>3</sup> Department of Computer Science <sup>4</sup> Department of Biostatistics & Bioinformatics

Duke University, NC, USA

{maciej.mazurowski, haoyu.dong151, hanxue.gu,  
jichen.yang, nicholas.konz, yixin.zhang7}@duke.edu

## Abstract

*Training segmentation models for medical images continues to be challenging due to the limited availability and acquisition expense of data annotations. Segment Anything Model (SAM) is a foundation model trained on over 1 billion annotations, predominantly for natural images, that is intended to be able to segment the user-defined object of interest in an interactive manner. Despite its impressive performance on natural images, it is unclear how the model is affected when shifting to medical image domains. Here, we perform an extensive evaluation of SAM’s ability to segment medical images on a collection of 11 medical imaging datasets from various modalities and anatomies. In our experiments, we generated point prompts using a standard method that simulates interactive segmentation. Experimental results show that SAM’s performance based on single prompts highly varies depending on the task and the dataset, i.e., from 0.1135 for a spine MRI dataset to 0.8650 for a hip x-ray dataset, evaluated by IoU. Performance appears to be high for tasks including well-circumscribed objects with unambiguous prompts and poorer in many other scenarios such as segmentation of tumors. When multiple prompts are provided, performance improves only slightly overall, but more so for datasets where the object is not contiguous. An additional comparison to RITM [19] showed a much better performance of SAM for one prompt but a similar performance of the two methods for a larger number of prompts. We conclude that SAM shows impressive performance for some datasets given the zero-shot learning setup but poor to moderate performance for multiple other datasets. While SAM as a model and as a learning paradigm might be impactful in the medical imaging domain, extensive research is needed to identify the proper ways of adapting it in this domain.*

## 1. Introduction

Image segmentation is a central task in medical image analysis, ranging from the segmentation of organs [17], abnormalities [3], bones [8], and others [13]. Deep learning has dramatically altered how task is performed and brought significant performance improvements in many domains [6, 15]. However, developing and training segmentation models for new medical imaging data and/or tasks is practically challenging, due to the expensive and time-consuming nature of collecting and curating medical images, primarily because trained radiologists must typically provide careful mask annotations for images.

These difficulties could be significantly lessened with the advent of foundation models [22] and zero-shot learning. Foundation models are neural networks trained on an extensive amount of data, using creative learning and prompting objectives that typically do not require traditional supervised training labels, both of which contribute towards the ability to perform zero-shot learning on completely new data. Foundation models have shown paradigm-shifting abilities in the domain of natural language processing [12]. A recently developed Segment Anything Model uses similar principles for image segmentation [9].

### 1.1. What is SAM?

Segment Anything Model is a segmentation model that aims at segmenting the user-defined object of interest when prompts are given. Prompts can take the form of a point, a set of points (including an entire mask), a bounding box, or text. The model is asked to return a valid segmentation mask even in the presence of ambiguity in the prompt. The general idea behind this approach is that the model learns the concept of an object and thus can segment any object that is pointed out. This results in a high potential for being able to segment objects of types that it has not seen without any additional training, i.e., high performance in the zero-

Abbreviated dataset name	Full dataset name and citation	Modality	Num. classes	Object(s) of interest	Num. images
MRI-Spine	Spinal Cord Grey Matter Segmentation Challenge [14]	MRI	2	Gray matter, spinal cord	551
MRI-Heart	Medical Segmentation Decathlon [18]	MRI	1	Heart	1,302
MRI-Prostate	Initiative for Collaborative Computer Vision Benchmarking [10]	MRI	1	Prostate	1,854
MRI-Brain	The Multimodal Brain Tumor Image Segmentation Benchmark (BraTS) [11]	MRI	3	Three parts of brain tumor	13,107
Xray-Chest	Montgomery County and Shenzhen Chest X-ray Datasets [7]	X-ray	1	Chest	704
Xray-Hip	X-ray Images of the Hip Joints [5]	X-ray	2	Ilium, femur	140
US-Breast	Dataset of Breast Ultrasound Images [2]	Ultrasound	1	Breast	780
US-Kidney	CT2US for Kidney Segmentation [20]	Ultrasound	1	Kidney	4,586
CT-Liver	The Liver Tumor Segmentation Benchmark (LiTS) [4]	CT	1	Liver	5,501
CT-Organ	CT Volumes with Multiple Organ Segmentations (CT-ORG) [17]	CT	6	Liver, bladder, lungs, kidney, bone, brain	4,776
PET-Liver	Y-90 PET/CT & SPECT/CT and Corresponding Contours Dataset 31JULY2020 [21]	PET/CT	1	Liver tumor	16

Table 1. **All datasets evaluated in this paper.** Note that for 3D modalities, “num. images” refers to the number of 2D slice images.

shot learning regime. In addition to the prompt-based definition of the task, the authors utilized a specific model architecture and a uniquely large dataset to achieve this goal, described as follows.

SAM was trained progressively alongside the development of the dataset (SA-1B). The dataset was developed in three stages. First, a set of images was annotated by human annotators by clicking on objects and manually refining masks generated by SAM which at that point was trained using public datasets. Second, the annotators were asked to segment masks that were not confidently generated by SAM to increase the diversity of objects. The final set of masks was generated automatically by prompting the SAM model with a set of points distributed in a grid across the image and selecting confident and stable masks.

## 1.2. How to segment medical images with SAM?

SAM is designed to require a prompt or a set of prompts to produce a segmentation mask. Technically, the model can be run without a prompt to provide any visible object, but there is not a high expectation for this to be useful in medical imaging, where there is usually some specific object of interest out of many in the image. Given this prompt-based nature, in its basic form, SAM cannot be used the same way

as most of segmentation models in medical imaging where the input is simply an image and the output is a segmentation mask or masks for the desired object or objects.

We propose that there are three main ways in which SAM can be used in the process of segmentation of medical images. The first two involve using the actual Segment Anything Model as is in the process of annotation, mask generation, or training of additional models. Those modes do not involve changes to SAM model. The third mode involves the process of training/fine-tuning a SAM-like model specifically designed for medical images. Note that we do not comment here on text-based prompting, as it is still in the proof-of-concept stage and might be of use in the future.

### Semi-automated annotation (“human in the loop”).

The manual annotation of medical images is one of the main challenges of developing segmentation models in this field since it typically requires the valuable time of physicians. SAM could be used in this setting as a tool for faster annotation. This could be done in different ways. In the simplest case, a human user provides prompts for SAM, which generates a mask to be approved or modified by the user. This could be done iteratively. Another option is where SAM is



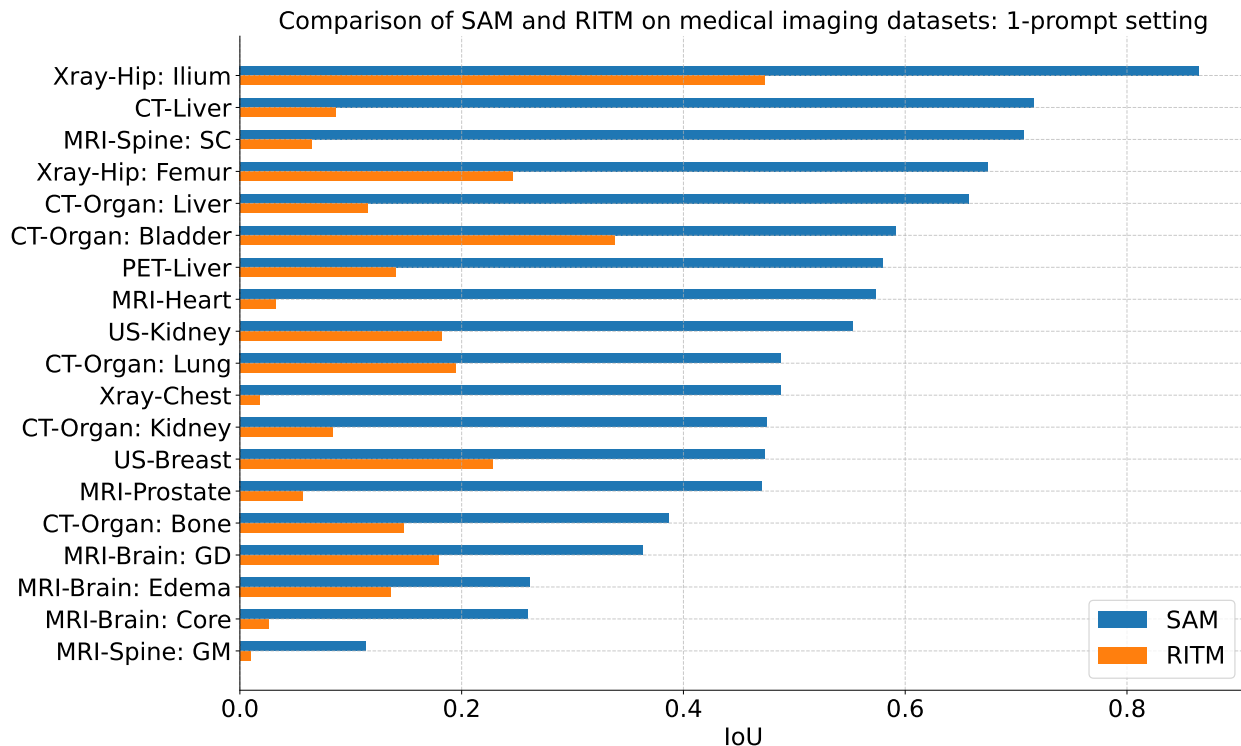


Figure 1. Accuracy of masks generated by SAM vs. RITM for single point prompting of different datasets and/or objects (Tab. 1).

given prompts distributed in a grid across the image, and generates masks for multiple objects which are then named, selected, and/or modified by the user. This is only the start; many other possibilities could be imagined.

**SAM assisting other segmentation models.** One version of this usage mode is where SAM works alongside another algorithm to automatically segment images (an “inference mode”). For example, SAM, based on point prompts distributed across the image, could generate multiple object masks which then could be classified as specific objects by a separate classification model. Similarly, an independent detection model [16] could generate object-bounding boxes of images to be used as prompts for SAM to generate precise segmentation masks.

Further, SAM could be used in the loop with a semantic segmentation model in the process of training such a model. For example, the masks generated by a segmentation model on unlabeled images during training could be used as prompts to SAM to generate more precise masks for these images, which could be used as iteratively refined supervised training examples for the model being trained. One could conceptualize many other specific modes of including SAM in the process of training new segmentation models.

## New medical image foundation segmentation models.

In this usage mode, the development process of a new segmentation foundation model for medical images could be guided by how SAM was developed. The largest difficulty of this would be in the much lower availability of medical images and quality annotations, compared to natural images, but this is possible in principle. A more feasible option could be to fine-tune SAM on medical images and masks from a variety of medical imaging domains, rather than training from scratch, as this would likely require fewer images.

## 2. Methodology

In the previous section, we described various usage scenarios of SAM for medical image segmentation. These are conceptually promising, yet still rely on the assumption that SAM can generate accurate segmentations of medical images. Here, we experimentally evaluate this claim and evaluate the performance of SAM within a variety of different realistic usage scenarios and datasets in medical imaging.

### 2.1. Datasets

We compiled and curated a set of 11 publicly available medical imaging datasets for image segmentation. While the phrase “medical imaging” is sometimes used to refer to

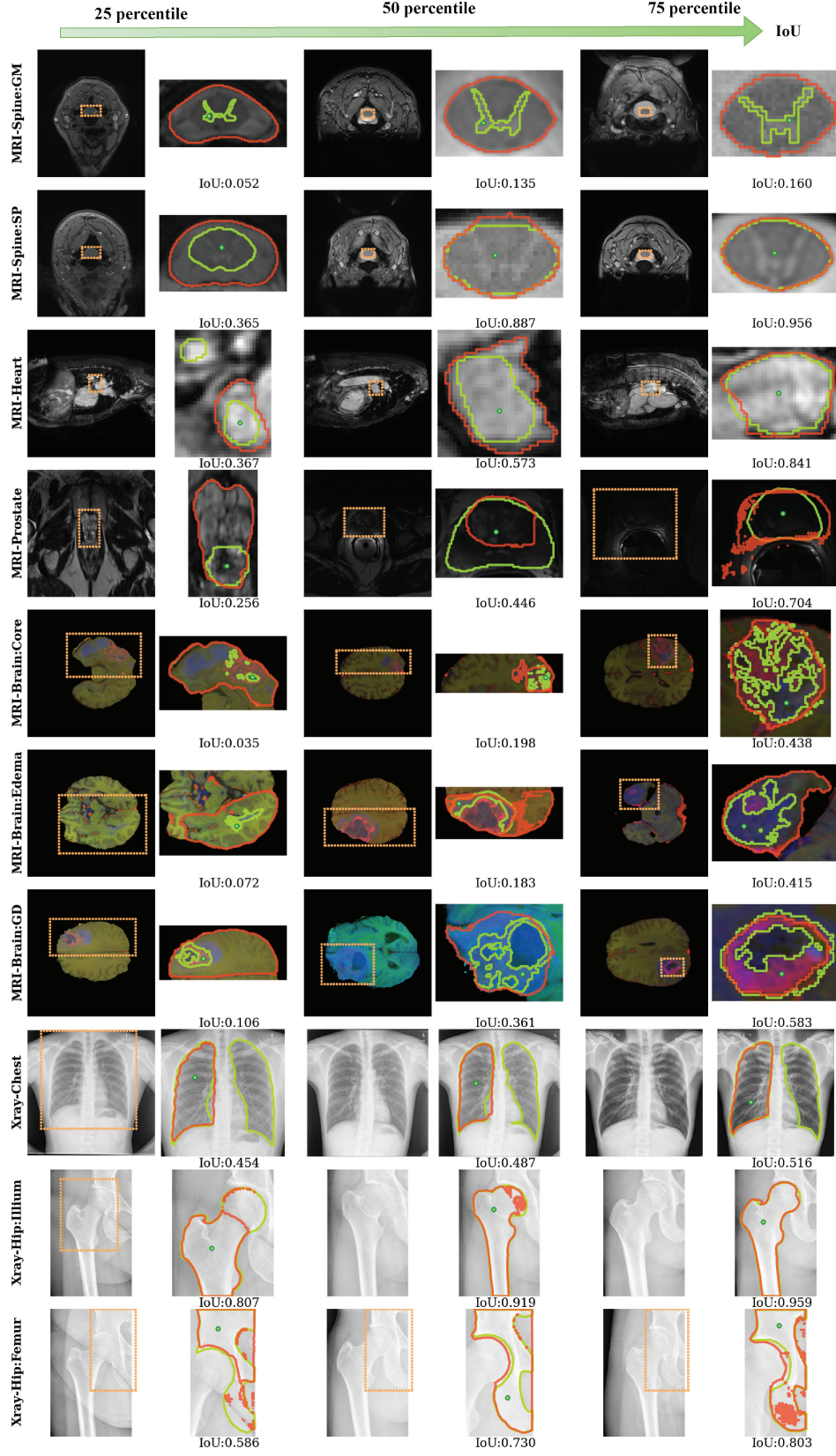


Figure 2. Examples of SAM’s segmentations of medical images (1 of 2; additional datasets shown in Fig. 3).

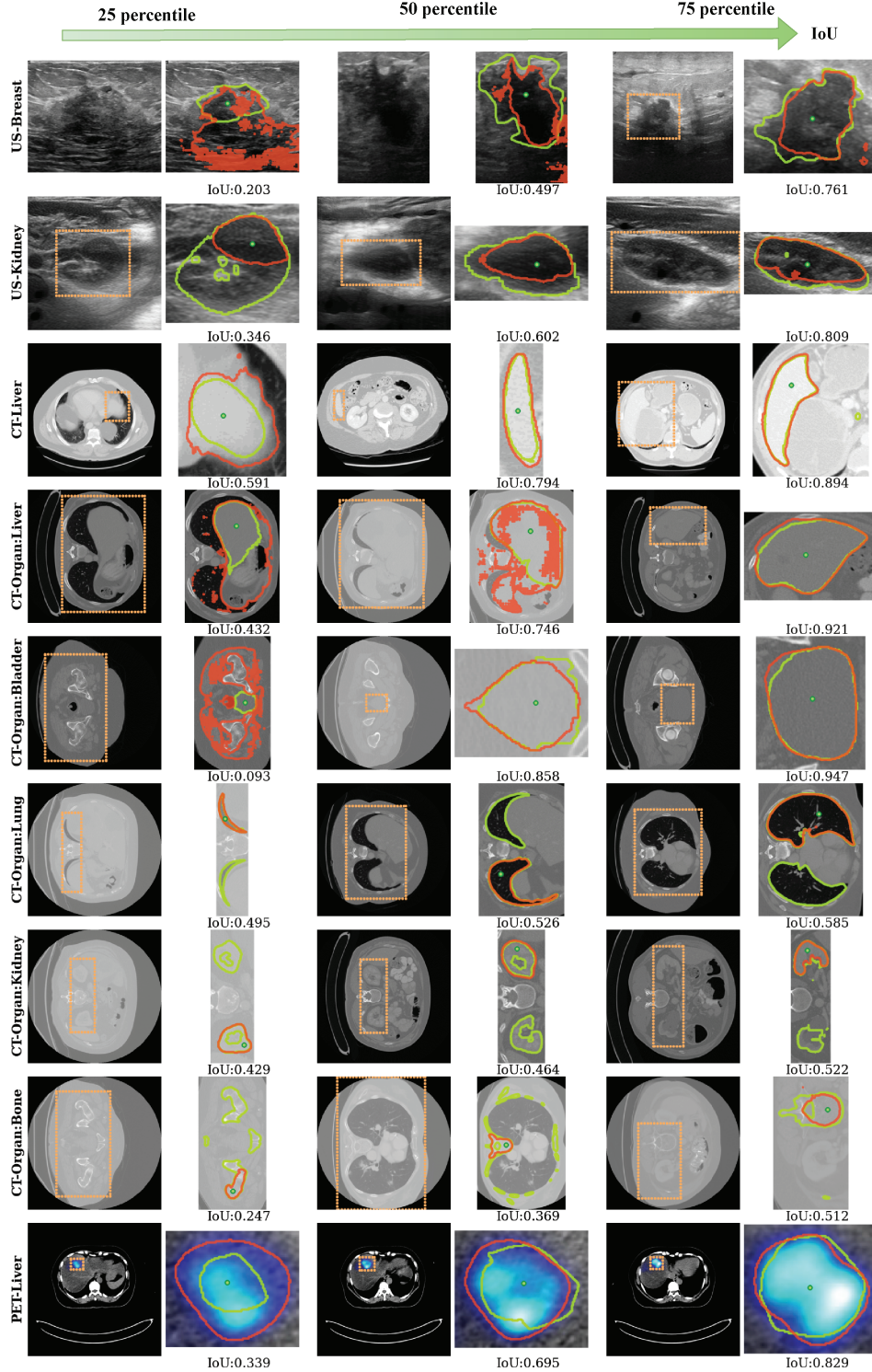


Figure 3. Examples of SAM’s segmentations of medical images (2 of 2; additional datasets shown in Fig. 2).

all images pertaining to medicine, we focus on the common definition meaning radiological images. Our dataset includes planar X-rays, magnetic resonance images (MRIs),

computed tomography (CT) images, ultrasound (US) images, and positron emission tomography (PET) images. The datasets are summarized in Table 1.



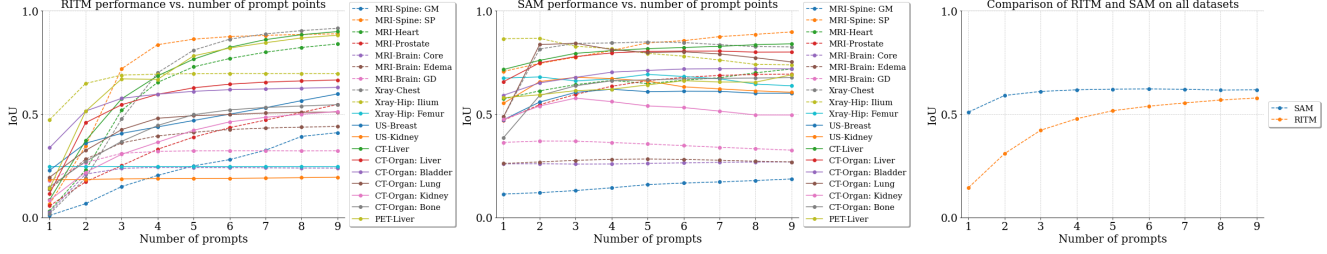


Figure 4. Comparing performances of SAM to RITM on different datasets and various numbers of prompts

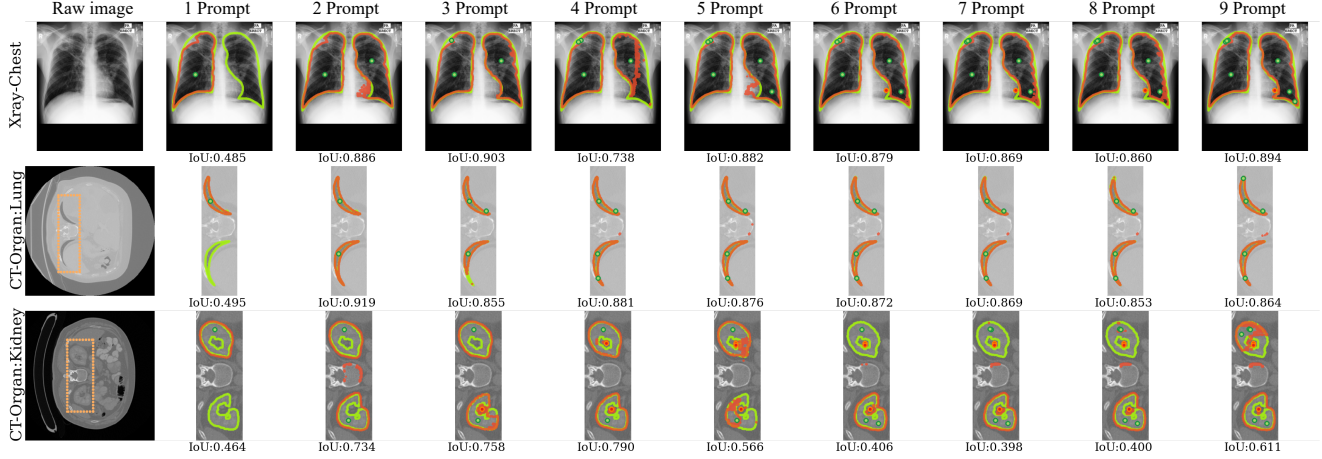


Figure 5. SAM performance on multi-region images with various numbers of prompts

## 2.2. Experiments

For each dataset, we evaluated the performance of SAM by creating one or more prompts per object and evaluating the accuracy of the masks that SAM generates with the prompts, with respect to the “ground truth” mask annotations for the given dataset and task. We always use the mask with highest confidence generated by SAM for a given prompt. We used a common, intuitive strategy for simulating realistic point prompt generation which reflects how those could be generated by a user in an interactive way. The details of the prompt generation is illustrated in Algorithm 1.

Following SAM’s procedure, we also select mIoU as the evaluation metric. However, empirical study shows that SAM’s performance can vary significantly among different classes of the same image. Therefore, we convert the multi-class prediction problem with  $N$  classes to  $N$  binary classification problems and thus it suffices to use IoU as the final evaluation metric.

## 3. Results

The performance of SAM and RITM for the single point prompt scenario are shown in Figure 1. The results demon-

strate overall moderate and database-dependent performance of SAM. The performance ranged from 0.2596 to 0.8649 except for the MRI-Spine:GM dataset where the performance was very low at  $\text{IoU}=0.1135$ .

Figures 2 and 3 show examples of segmentations generated in the single-point prompt scenario. For each dataset (the rows; names are furthest to the left), we provide examples of segmentations in the 25th, 50th, and 75th percentile of accuracy/mIoU (the columns) for a given dataset. Green contours represent the ground truth masks, red contours represent SAM’s prediction, and green points represent the first positive prompt given to SAM. This figure illustrates a high variability of SAM’s performance ranging from near-perfect for well-circumscribed objects with unambiguous prompts to very poor, particularly for objects with ambiguous prompts. Note also that lower performance is sometimes a reflection of the fact that the object of interest is not contiguous and SAM segments only one part of the objects (sometimes very accurately).

The performance of SAM and RITM for the multi-prompt scenario is shown in Figure 4. SAM has a much higher performance when there is only one prompt, but the difference between the two decreases as the number of prompts increases until the performance of the two becomes

---

**Algorithm 1** Prompt Point Generation Scheme

---

**Input:** Image  $X \in \mathbb{R}^{H \times W}$ , ground truth mask  $M \in \{0, 1\}^{H \times W}$ , Segment Anything Model SAM, prompt count  $N$ , closest-zero-pixel distance function  $d = \text{distanceTransform}()$  from OpenCV [1].

- 1: Initialize first prompt point  $p_1$  as the point within the mask foreground farthest from the background:
  - 2:  $\mathcal{P} = \underset{(i,j)}{\operatorname{argmax}}(d[(i,j), (k,l)])$  for all  $(i,j), (k,l)$  such that  $M_{ij} = 1, M_{kl} = 0$ .
  - 3: Choose randomly if multiple points satisfy this:
  - 4:  $p_1 = \text{random\_choice}(\mathcal{P})$
  - 5: Predict mask  $Y_1 = \text{SAM}(X, p_1)$
  - 6: Get prediction error region  $E_1 = Y_1 \cup M - Y_1 \cap M$
  - 7: Subsequent prompt points are those farthest from the boundary of iteratively-updating error region  $E_n$ :
  - 8: **for**  $n = 2, \dots, N$  **do**
  - 9:  $\mathcal{P}_n = \underset{(i,j)}{\operatorname{argmax}}(d[(i,j), (k,l)])$  for all  $(i,j), (k,l)$  such that  $[E_{n-1}]_{ij} = 1, [E_{n-1}]_{kl} = 0$ .
  - 10:  $p_n = \text{random\_choice}(\mathcal{P}_n)$
  - 11:  $Y_n = \text{SAM}(X, p_n)$
  - 12:  $E_n = Y_n \cup M - Y_n \cap M$
  - 13: **end for**
  - 14: **return** Prompt points  $p_1, \dots, p_N \in \mathbb{N}^2$
- 

very close for 9 prompts.

As shown in Figure 5, SAM with one prompt is having a hard time completing multi-region tasks. It is more likely to segment one single and continuous region instead of trying to find more semantically similar regions on the entire image. For example, lung segmentation (row 2 of fig. 5) normally contains two parts of the lung, but SAM often segments only one part with one prompt. With an increasing number of prompts, it is more likely that all regions will be successfully prompted to SAM, and the segmentation performance will increase substantially. However, as shown in row 3 of Fig. 5, too many prompts might also damage the performance.

## 4. Conclusions

In this study, we evaluated the new Segment Anything Model for the segmentation of medical images. We found that the model segmentation accuracy is overall moderate and varies significantly across different datasets and different cases. This demonstrates the potential promise of SAM within the context of medical imaging but also shows that the model cannot be applied in the context of medical imaging with high confidence as is. Also, as most medical images are shown as 3D formatting, future analysis on extending it to a 3D version is worth exploring.

## References

- [1] OpenCV: Miscellaneous Image Transformations. 7
- [2] Walid Al-Dhabyani, Mohammed Gomaa, Hussien Khaled, and Aly Fahmy. Dataset of breast ultrasound images. *Data in brief*, 28:104863, 2020. 2
- [3] Syed Muhammad Anwar, Muhammad Majid, Adnan Qayyum, Muhammad Awais, Majdi Alnowami, and Muhammad Khurram Khan. Medical image analysis using convolutional neural networks: a review. *Journal of medical systems*, 42:1–13, 2018. 1
- [4] Patrick Bilic, Patrick Christ, Hongwei Bran Li, Eugene Vorontsov, Avi Ben-Cohen, Georgios Kaissis, Adi Szeskin, Colin Jacobs, Gabriel Efrain Humpire Mamani, Gabriel Chartrand, et al. The liver tumor segmentation benchmark (lits). *Medical Image Analysis*, 84:102680, 2023. 2
- [5] Daniel Gut. X-ray images of the hip joints. 1, July 2021. Publisher: Mendeley Data. 2
- [6] Mohammad Hesam Hesamian, Wenjing Jia, Xiangjian He, and Paul Kennedy. Deep learning techniques for medical image segmentation: achievements and challenges. *Journal of digital imaging*, 32:582–596, 2019. 1
- [7] Stefan Jaeger, Sema Candemir, Sameer Antani, Yi-Xiang J Wang, Pu-Xuan Lu, and George Thoma. Two public chest x-ray datasets for computer-aided screening of pulmonary diseases. *Quantitative imaging in medicine and surgery*, 4(6):475, 2014. 2
- [8] Baris Kayalibay, Grady Jensen, and Patrick van der Smagt. Cnn-based segmentation of medical imaging data. *arXiv preprint arXiv:1701.03056*, 2017. 1
- [9] Alexander Kirillov, Eric Mintun, Nikhila Ravi, Hanzi Mao, Chloe Rolland, Laura Gustafson, Tete Xiao, Spencer Whitehead, Alexander C Berg, Wan-Yen Lo, et al. Segment anything. *arXiv preprint arXiv:2304.02643*, 2023. 1
- [10] Guillaume Lemaître, Robert Martí, Jordi Freixenet, Joan C Vilanova, Paul M Walker, and Fabrice Meriaudeau. Computer-aided detection and diagnosis for prostate cancer based on mono and multi-parametric mri: a review. *Computers in biology and medicine*, 60:8–31, 2015. 2
- [11] Bjoern H Menze, Andras Jakab, Stefan Bauer, Jayashree Kalpathy-Cramer, Keyvan Farahani, Justin Kirby, Yuliya Burren, Nicole Porz, Johannes Slotboom, Roland Wiest, et al. The multimodal brain tumor image segmentation benchmark (brats). *IEEE transactions on medical imaging*, 34(10):1993–2024, 2014. 2
- [12] OpenAI. Gpt-4 technical report, 2023. 1
- [13] Dzung L Pham, Chenyang Xu, and Jerry L Prince. Current methods in medical image segmentation. *Annual review of biomedical engineering*, 2(1):315–337, 2000. 1
- [14] Ferran Prados, John Ashburner, Claudia Blaiotta, Tom Brosch, Julio Carballido-Gamio, Manuel Jorge Cardoso, Benjamin N Conrad, Esha Datta, Gergely Dávid, Benjamin De Leener, et al. Spinal cord grey matter segmentation challenge. *Neuroimage*, 152:312–329, 2017. 2
- [15] Muhammad Imran Razzak, Saeeda Naz, and Ahmad Zaib. Deep learning for medical image processing: Overview, challenges and the future. *Classification in BioApps: Automation of Decision Making*, pages 323–350, 2018. 1



- [16] Shaoqing Ren, Kaiming He, Ross Girshick, and Jian Sun. Faster r-cnn: Towards real-time object detection with region proposal networks, 2016. [3](#)
- [17] Blaine Rister, Kaushik Shivakumar, Tomomi Nobashi, and Daniel L. Rubin. CT-ORG: A Dataset of CT Volumes With Multiple Organ Segmentations, 2019. Version Number: 1 Type: dataset. [1](#), [2](#)
- [18] Amber L Simpson, Michela Antonelli, Spyridon Bakas, Michel Bilello, Keyvan Farahani, Bram Van Ginneken, Annette Kopp-Schneider, Bennett A Landman, Geert Litjens, Bjoern Menze, et al. A large annotated medical image dataset for the development and evaluation of segmentation algorithms. *arXiv preprint arXiv:1902.09063*, 2019. [2](#)
- [19] Konstantin Sofiiuk, Ilya A. Petrov, and Anton Konushin. Reviving iterative training with mask guidance for interactive segmentation. *2022 IEEE International Conference on Image Processing (ICIP)*, pages 3141–3145, 2021. [1](#)
- [20] Yuxin Song, Jing Zheng, Long Lei, Zhipeng Ni, Baoliang Zhao, and Ying Hu. Ct2us: Cross-modal transfer learning for kidney segmentation in ultrasound images with synthesized data. *Ultrasonics*, 122:106706, 2022. [2](#)
- [21] BJ Van and YK Dewaraja. Y-90 pet/ct & spect/ct and corresponding contours dataset 31july2020. *University of Michigan-Deep Blue Data*, 2020. [2](#)
- [22] Ce Zhou, Qian Li, Chen Li, Jun Yu, Yixin Liu, Guangjing Wang, Kai Zhang, Cheng Ji, Qiben Yan, Lifang He, et al. A comprehensive survey on pretrained foundation models: A history from bert to chatgpt. *arXiv preprint arXiv:2302.09419*, 2023. [1](#)